49th AIAA Aerospace Sciences Meeting including the New Horizons Forum and Aerospace Exposition
4 - 7 January 2011, Orlando, Florida

AIAA 2011-1139

Laser Supported Detonation in Argon Atmosphere

Kohei Shimamura[1], Keisuke Michigami[1], Bin Wang[1], Kimiya Komurasaki[2]
The University of Tokyo, Kashiwa, Chiba 277-8561, JAPAN

and

Yoshihiro Arakawa[3]
The University of Tokyo, Bunkyo Tokyo 113-8656, JAPAN

Characteristics of Laser supported detonation (LSD) and the induced plasma were measured in argon atmosphere using Schlieren graph method and emission spectroscopy. The results revealed that the peak electron density and temperature were, respectively, about 1.0×10^{25} m^{-3} and 5.8×10^{4} K in argon and 8.0×10^{22} m^{-3} and 3.8×10^{4} K in air. Furthermore, a number of ionizing collision of ~ 10^{-7} W in the laser absorption both argon and air atmosphere were measured at LSD termination. Result reveals that the LSD termination in argon has a much longer time to propagate than in air. It might be depend on the electron temperature and density behind the shock wave.

I. Introduction

Laser induced plasma and resulting strong shock wave have been attracting interests for laser propulsion[1-5]. Understanding Laser Supported Detonation is a key to improving the design of laser energy propulsion, and the influence of gas species might give the key to elucidate for LSD. Argon gas is one of the inert gases and its ionization and excitation processes are simple comparing with air.

The LSD (Fig.1 (a)) is schematically expressed in Fig.1 (b). A peak of electron temperature T_e and density n_e is observed in a plasma layer behind the shock wave. Although T_e and n_e decreased as getting close to the shock wave, n_e was nonzero at the shock front. One hypothesis states that photo-ionization induced by UV radiation from the plasma layer behind the shock wave generates seed electrons for the precursor layer. The Bremsstrahlung radiation energy W_{rad} (W/m^3), which can contribute to single-photon ionization ahead of the shock wave, is expressed as[6],

[1] Graduate student, Department of Advanced Energy, The University of Tokyo.

[2] Professor, Department of Advanced Energy, The University of Tokyo, Senior Member.

[3] Professor, Department of Aeronautics and Astronautics, The University of Tokyo, Senior Member

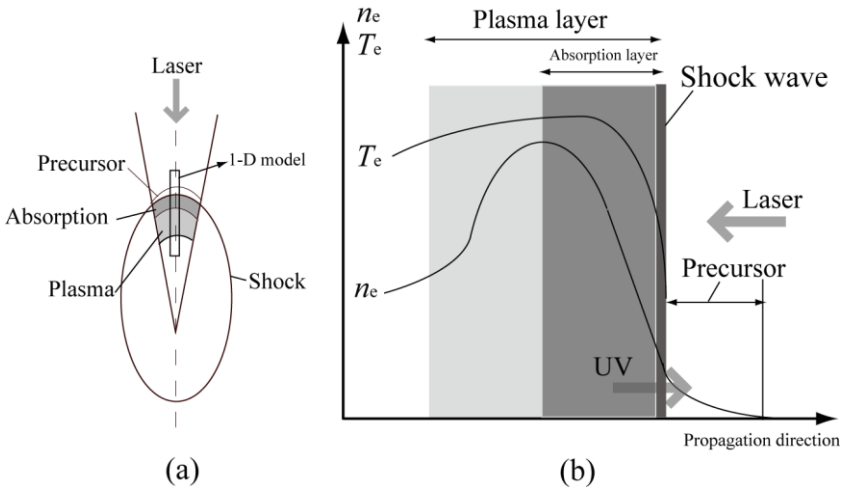

Figure 1 Model of the LSD wave in the laser plasma (a) and one-dimensional for the LSD (b).

$$W_{\mathrm{rad}} = \int_{\nu_{\mathrm{i}}}^{\infty} w(\nu)d\nu = 6.3\times10^{-53}\sqrt{\frac{e}{kT_{\mathrm{e}}}}n_{\mathrm{e}}n_{\mathrm{i}}\frac{kT_{\mathrm{e}}}{h}\exp\left(-\frac{h\nu_{\mathrm{i}}}{kT_{\mathrm{e}}}\right). \quad (1)$$

This formula is derived from the Rutherford scattering. Here, ν_{i} is the threshold frequency, which is related to the wavelength 75.2 nm for argon and 102.5 nm for air, the ionization threshold of argon, n_{i}, h and k represent the number density of ions, Planck's constant and the Boltzmann's constant, respectively. The photo-ionization phenomena, apparently, depend on n_{e} and T_{e} and might be related to the precursor of the LSD. The objectives of this study are to evaluate photo-ionization ahead of the LSD and to discuss about the LSD termination conditions.

In terms of the gas discharge physics, the structure of a streamer might give the elucidation for the propagation of LSD. The streamer is a moderately weakly ionized thin channel formed from the primary avalanche in the strong electric field, which grows toward one or both the electrodes[7]. It is well known that the streamer grows toward the anode or cathode, which are said to be negative or positive streamer. In the present case, the laser beam produces the strong electric field and the LSD wave propagates toward the laser beam. Furthermore, there are no electrodes, the front of LSD wave, thus, is thought to be the negative streamer. The early assumption of physical model for streamer by Loeb[8] was incorporated into the three-dimensional of the propagation structure[9]. The streamer is assumed to be a symmetrical cylinder and the master formulas for propagation are Poisson equation and the continuity of electron and ion density. One of the most interesting phenomena, which are similarity with LSD, occurs in the streamer head. The streamer develops toward the electrodes due to the photoionization in the vicinity of tip.

In our previous study, the characteristic of the laser induced plasma was investigated, such as the energy conversion efficiency and threshold laser power density, which were mainly investigated by a CO_2 laser[14-16]. Recently, the development of a high-power glass laser makes the application possibility for the laser propulsion. A Nd:Glass laser was used in the present study. We measured the LSD termination, n_{e} and T_{e} using the emission

spectroscopy and the Schlieren graph and estimated a number of ionizing collisions $W_{rad}V_r$ behind the shock wave around the LSD termination time using the simpler formula.

II. Temporal Evolution of the Blast Wave in Argon Atmosphere

According to the theory of streamer propagation, the propagation of ionization wave might depend on the ambient gas. In the LSD regime, the blast wave and the ionization wave develop along the laser beam axis together. It is assumed that the different gas species make a difference for the propagation of LSD wave. Figure 2 shows the setup of the Schlieren graph method. A Nd:Glass laser used in the present study is the same as it in the former study[17]. The laser produces a pulse of 33 ns pulse width at 1,053 nm. Temporal laser power profiles obtained using a photodetector and the details terms of this laser are presented in the Fig.4. A beam of 40 mm in diameter was focused by a 6.3 *f* - number lens and a beam expander inside a vacuum chamber. The chamber was filled with argon gas at 101.3 kPa after evacuation by a rotary vacuum pump. A YAG laser (CW, 532 nm, 1.0 W) was used as probe light. It projects the pictures of plasma on a high-speed ICCD camera (Ultra 8; DRS Technology Inc.) that enables us to take 8 frames in each laser pulse at a framing rate up to 100 million fps with the minimum exposure time of 10 ns. The synchronization between the ignition and the photographing is mainly controlled by a delay generator, which firstly receives a trigger signal came from the Nd:Glass laser, then after regulating and adding a adjustable delay, sent the trigger signal to the camera. The energy meter was used to monitor the incident pulse laser energy; the energy fluctuation was controlled in $\pm$5 %. Figure 3 gives the pictures of the plasma at t = 0.38 to 3.38 μs, where t is the elapsed time after laser initiation.

Figure 4 portrays the shock front and the ionization frond displacements in argon gas along the laser axis. The displacements of the two fronts coincide with each other during the LSD regime. The point of intersection of these two curves indicates timing of the LSD termination at 800 ns. This termination time in air was observed at 300 ns in the previous study. Furthermore, the comparison with air and argon is observed on the displacement of the blast wave. The velocity of the blast wave in both of gases are estimated at 1.76 $\times 10^3$ m/s for air and 1.94 $\times 10^3$ m/s for argon. In order to consider the ambient gas, a Mach-number, divided by the sound velocity, are also estimated at 5.23 for air and 6.22 for argon. These results indicate that the propagation of LSD depends on the ambient gas species.

III. Measurement of the Electron Density and Temperature

To evaluate the number of electron density and the electron temperature, the emission spectroscopy for

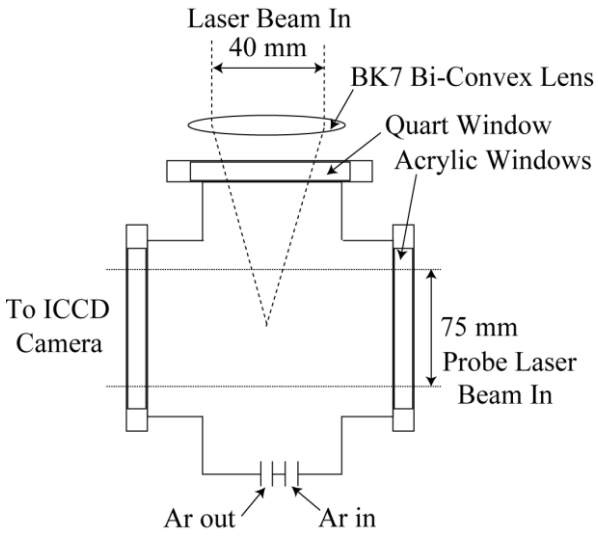

Figure 2 Schematic of the schlieren graph system.

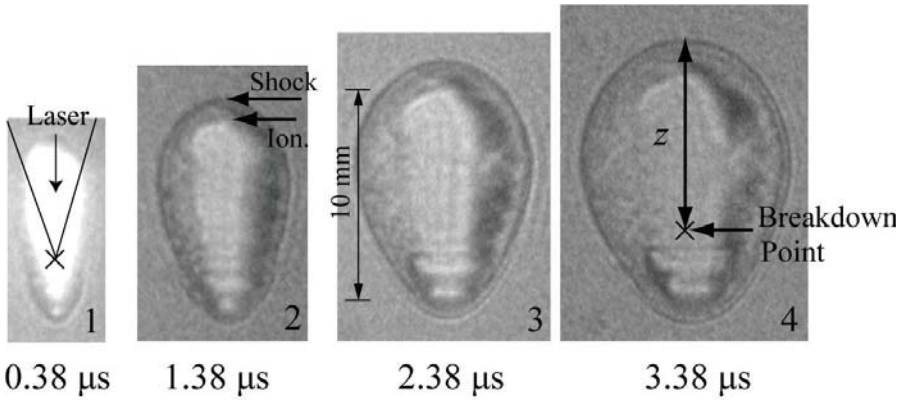

Figure 3 Schlieren graph of the laser induced plasma. Each picture taken in 101.3 kPa, E = 1.0 J, f = 6.3 and laser wavelength 1,053 nm. All of the pictures are same scale ratio.

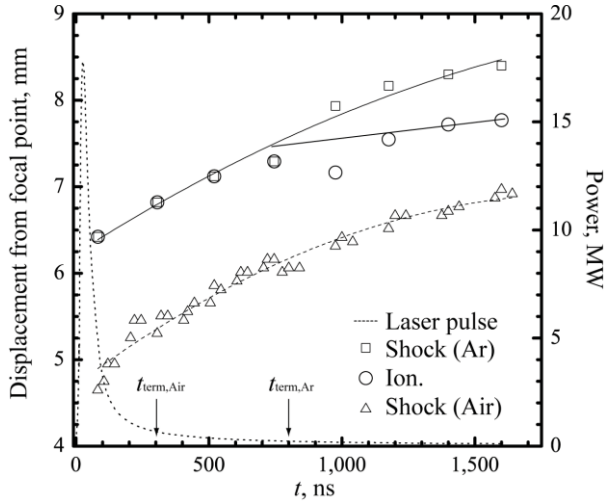

Figure 4 Temporal changes of the displacements of the shock front and the ionization front (dashed line) from the focal point and the laser power (dot-line). LSD termination time is indicated by arrows. p = 101.3 kPa, E = 1.0 J, f = 6.3 and laser wavelength 1,053 nm.

Ar^+ and N^+ are used. Figure 5 portrays a schematic of the emission spectroscopy experiment. The irradiance of the plasma is collected and analyzed using a Mechelle spectrometer (Aryelle200; LTB Inc.) whose spectral resolution $\lambda/\Delta\lambda$ is 8,000 in the range of wavelength from 250 nm to 900 nm. During the initial stages, especially < 600 ns, the time integrated intensifiers are 30 ns. Calibration of wavelength was done using a Hg-lamp in the spectrometer and the calibration of sensitivity was done using a halogen lamp. From the emission spectrum of the laser induced plasma, the information of T_e and n_e can be inferred using, respectively, the Boltzmann plot and the Stark broadening. It is reasonable to assume that the laser induced plasma is to be in the local thermodynamics equilibrium and we determine the electron temperature from several spectral lines (see Table 1. [18]), where A_{ik} is the transition probability, E_k represents the upper level energy and g_k stands for the upper statistical weight. The full width of half maximum of a Stark broadening $\Delta\lambda_{stark}$ is calculated as[19],

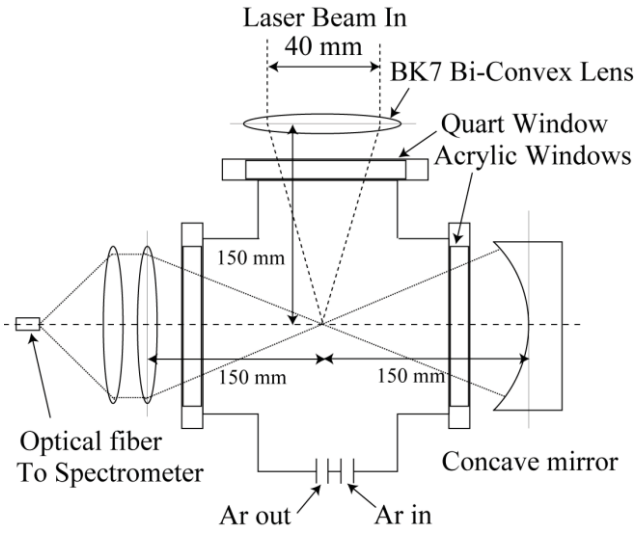

Figure 5 Schematic of the spectroscopy system.

$$\Delta\lambda_{\text{stark}} = 2W\left(\frac{n_e}{10^{15}}\right). \quad (2)$$

where W is the electron-impact half width, which was obtained from Griem[19]. The measurements of electron density were deduced from the Ar^+ line at 480.6 nm and the N^+ five-lines. Figures 6 (a) and (b) present the examples of applying these method at the time of t = 520 ns for Ar^+. Consequently, Fig. 7 gives the time dependency of T_e and n_e for spectral line fitting the Voigt function (for Ar II and N II). A necessary criterion of the LTE assumption is given by the relation[20],

$$n_e \geq 1.4\times10^{14} T_e^{0.5}(E_k - E_i)^3 \quad .(3)$$

In the present study, the largest parameters of the temperature and the energy gap are, respectively, 5.0 eV and 2.8 eV and the smallest density is 5.1×10^{24} m^{-3}. As a result of estimation, using Eq.(3), the light hand side is 6.9×10^{24} m^{-3} and then all of the data we observed are higher than this limit. All of the date for air are also sufficient this condition.

In the beginning stage, $n_e = 1.0\times10^{25}$ m^{-3} and $T_e = 5.8\times10^4$ K for argon laser plasma at t = 0.3 μs are observed. Besides, $n_e = 8.0\times10^{22}$ m^{-3} and $T_e = 3.8\times10^4$ K for air laser plasma at t = 0.2 μs are investigated. Both of n_e and T_e decrease with time as a reciprocal curve. At later stage around the LSD termination, n_e and T_e were estimated 6.0×10^{24} m^{-3} and 2.5×10^4 K for argon laser plasma at t = 0.8 μs and 7.0×10^{22} m^{-3} and 3.6×10^4 K for air plasma at t = 0.3 μs, respectively.

Table 1. Spectral line data for Ar II and N II from NIST[18]

	λ (nm)	A_{ik} (10^7 s^{-1})	E_k (eV)	g_k
Ar II	440.0986	3.04	19.22	6
	454.5052	4.71	19.87	4
	476.4865	6.4	19.87	4
	480.6020	7.80	19.22	6
	484.7810	8.49	19.31	2
	487.9864	8.23	19.68	6
N II	391.900	6.76	23.57	3
	395.585	1.31	22.00	5
	399.500	13.5	22.00	5
	444.703	11.4	23.20	5
	504.510	3.42	20.94	3

IV. The Rate of Ionization Collision behind the Shock Wave

The volume involved in radiation layer V_r (m^3) can be expressed as[15],

$$V_r = \frac{\pi}{3}\left(\frac{1}{2f}\right)^2\left\{z^3 - (z-\Delta z)^3\right\} \cong \frac{\pi\cdot z^2\Delta z}{4f^2}, \quad (4)$$

where f is the focusing number, r stands for the LSD wave-surface radius and z expresses the LSD wave displacement along the laser light channel from the

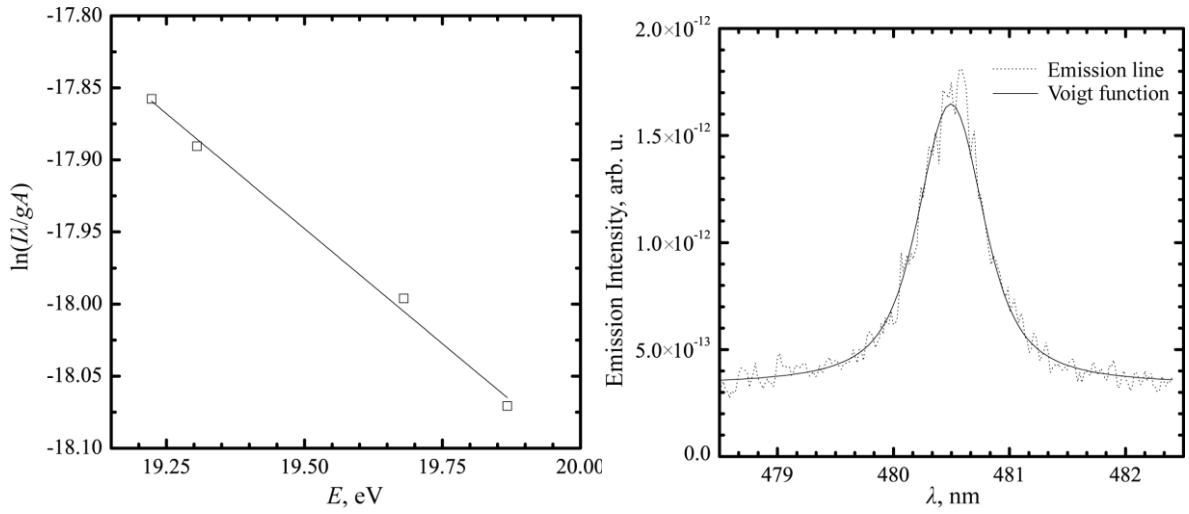

Figure 6 (a) Boltzmann plot for Ar^+ lines (left side) and (b) Stark broadening of Ar^+ 480.6 nm (right side) at t = 0.5 μs. The smooth curves (straight line) represent the fitted voigt curves. All other experimental manner are similar to these figures.

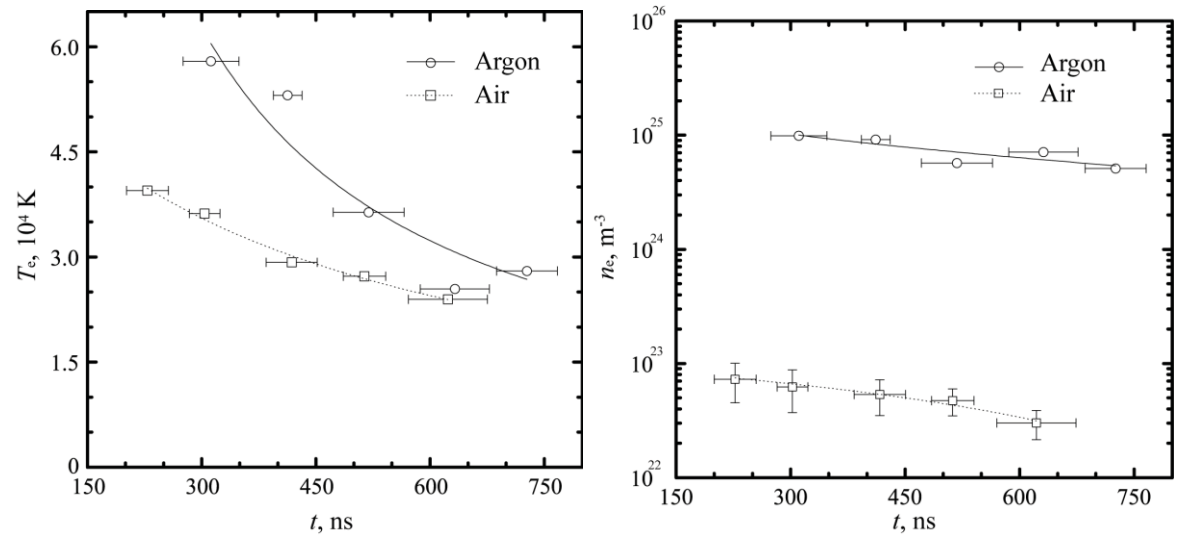

Figure 7 Temporal variation of the electron temperature (Left side) of the laser plasma after the laser spark. An Open square with dot line and open circle with dot-line are air and argon gas, respectively.

Figure 8 Temporal variation of the electron density (Right side). All of data plots are similarly to Fig.7.

focus, as shown in Fig.9 (a). The low angle of laser light channel (2.3 degrees) enables to suppose the approximation model, as show in Fig. 9 (b). In this case, Δz is assumed to be 1 mm[16]. The number of ionizing collision for argon and air are shown in Fig.10. The number of ionizing collision $W_{rad}V_r$ of ~ 10^{-7} W in the laser absorption layer for both argon and air were measured around the LSD termination. Each data plot in argon atmosphere appears to have even high value than in air. This makes sense because the Bremsstrahlung radiation energy depends on the electron temperature and density, and these parameters for the argon breakdown data were slightly higher than that for the air

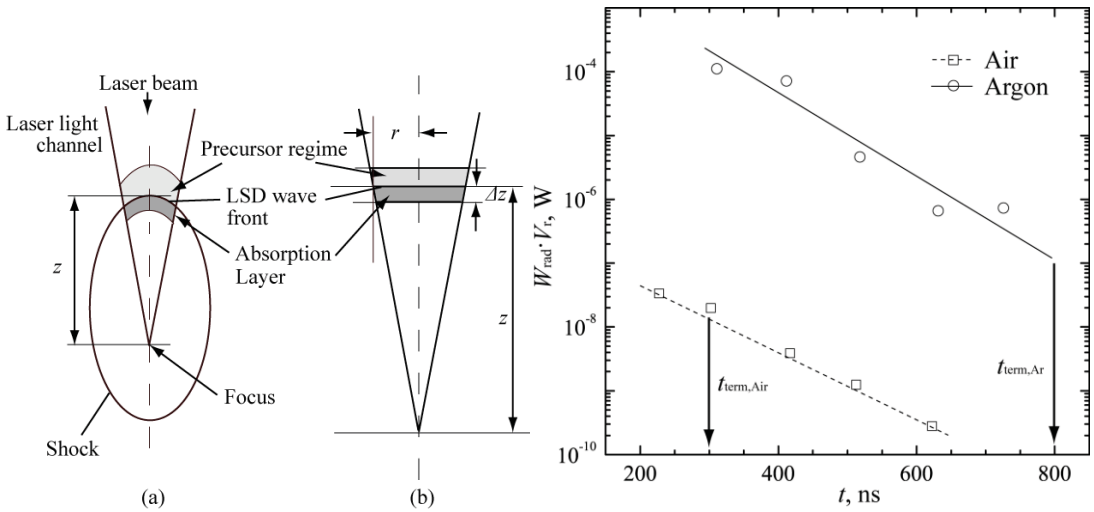

Figure 9 (a) Schematic and (b) approximation model for the LSD wave (Left side).

Figure 10 The number of ionizing collision in absorption layer for argon and air. (Right side) An Open square with dot-line and open circle with straight line are air and argon gas, respectively.

breakdown data. Further research and analysis will be needed to explain the photoionization phenomena reported here.

V. Summary

Focusing a Glass laser beam in argon atmospheres induced a blast wave. Measured the value of n_e and T_e at around the LSD termination were observed, respectively, 6.0×10^{24} m^{-3} and 2.5 $\times10^{4}$ K in argon atmosphere (t = 0.8 μs) and 7.0×10^{22} m^{-3} and 3.3×10^{4} K in air (t = 0.3 μs). From estimation using the relations presented herein, the number of ionizing collision of ~ 10^{-7} W in the laser absorption both argon and air atmosphere were measured around the LSD termination. The present study investigates that the both of electron temperature and density in the argon laser plasma behind the shock wave were higher than in air plasma. This is mainly because the LSD in argon atmosphere had a much longer time to maintain than in air.

Acknowledgements

This work is supported by a Grant-in-Aid for Scientific Research (a), No. 19296987, sponsored by the Ministry of Education, Culture, Sports, Science and Technology, Japan.

References

[1]Kantrowitz, A., "Propulsion to Orbit by Ground Based Lasers, Aeronaut. Astronaut. 10, 74 (1972).

[2]Myrabo, L.M., Messitt, D.G. and Mead, F. B., "Ground and Flight Tests of a Laser Propelled Vehicle, AIAA Paper, 98-1001 (1998).

[3]Mori, K., Komurasaki, K. and Arakawa, Y., "Nozzle Scale Optimum for the Impulse Generation in a Laser Pulsejet, J. Spacecr. Rockets 41, 887 (2004).

[4]Katsurayama, H., Komurasaki, K., Hirooka, Y., Mori, K. and Arakawa, Y.,"Numerical analyses of exhaust and refill processes of a laser pulse jet," J. Propul. Power 24, 999 (2008).

[5]Katsurayama, H., Komurasaki, K., and Arakawa, Y., "A preliminary study of pulse-laser powered orbital launcher,"Acta Astronautica 65, 1032 (2009).

[6]Kato, S., Takahashi, E., Sasaki , A. and Kishimoto, Y., "Theory and Simulation Models Including Atomic and Molecular Process", J. Plasma Fusion Res. 84(8). Pp.447-485 (2008).

[7]Raizer, Y. P., *Gas Discharge Physics*, Springer, Berlin, 1991.

[8]Loeb, L. B., *Basic Processes of Gaseous Electronics*, University of California Press, Berkeley, CA 1960.

[9]Bityurin, V.A. and Vedenin, P. V. "Electrodynamic model of a microwave streamer," Technical Physics Letters 35, 622-625 (2009)

[10]Zheleznyak, M. B., Mnatsakanyan, A. K. and Sizykh, S. V. "PHOTO-IONIZATION OF NITROGEN AND OXYGEN MIXTURES BY RADIATION FROM A GAS-DISCHARGE," High Temperature 20, 357-362 (1982)

[11]Kulikovsky, A. A. "The role of photoionization in positive streamer dynamics," Journal of Physics D-Applied Physics 33, 1514-1524 (2000)

[12]Penney, G. W. and Hummert, G. T. "PHOTOIONIZATION MEASUREMENTS IN AIR, OXYGEN, AND NITROGEN," Journal of Applied Physics 41, 572-& (1970)

[13]Naidis, G. V. "On photoionization produced by discharges in air," Plasma Sources Science & Technology 15, 253-255 (2006)

[14]Mori, K., Komurasaki, K. and Arakawa, Y., "Influence of the Focusing f Number on the Heating Regime Transition in Laser Absorption Waves", Journal of Applied Physics, Vol. 15, 2002, pp.5663-5667.

[15]Mori, K., Komurasaki, K. and Arakawa, Y.," Energy Transfer from a Laser Pulse to a Blast Wave in Reduced Pressure Air Atmospheres", Journal of Applied Physics, Vol 95, 2004, pp.5979-5983.

[16]Ushio, M., Kawamura, K., Komurasaki, K. and Arakawa, Y., "Effect of laser supported detonation wave confinement on termination conditions", Shock waves, Vol. 18, 2008, pp.155-157.

[17]Wang, B., Komurasaki K., Yamaguchi T., Shimamura K. and Arakawa Y., "Energy conversion in a Glass-laser-induced blast wave in air", Journal of Applied Physics, (to be published).

[18]NIST Atomic Spectra Database, http://physics.nist.gov.

[19]Griem H. R., *Plasma Spectroscopy*, McGraw-Hill, New York, 1964.

[20]Bekefi, G., *Principle of Laser Plasmas* (Wiley-Interscience, New York, 1976).

[21]Harilal, S.S., "Spatial and temporal evolution of argon sparks", Applied Optics, Vol.43, No.19, pp3931-3937.